New Insight into the Three-Coordinate Divalent Germanium Compounds $L^2GeΣ$ (L^2 = PhNC(Me)CHC(Me)NPh, Σ = Cl, I, Me, OMe). Structural, Photoelectron Spectroscopic, and Theoretical Analysis

Isabelle Saur,[†] Karinne Miqueu,[†] Ghassoub Rima,[†] Jacques Barrau,*[,†] Virginie Lemierre,[‡] Anna Chrostowska,[‡] Jean-Marc Sotiropoulos,[‡] and Geneviève Pfister-Guillouzo*[,‡]

Hétérochimie Fondamentale et Appliquée, UMR 5069, Université Paul Sabatier, 118, route de Narbonne, F-31062 Toulouse Cedex 4, France, and Laboratoire de Physico-Chimie Moléculaire, UMR 5624, Université de Pau et des Pays de l'Adour, Av. de l'Université, BP 1155, F-64013 Pau Cedex, France

Received March 4, 2003

An experimental and theoretical study of the heteroleptic divalent germanium compounds containing the bidentate coordinating monoanionic β-diketiminate ligand $L^2GeΣ$ (L^2 = PhNC(Me)CHC(Me)NPh; Σ = Cl (**1**), I (**2**), Me (**3**), OMe (**4**)) has been performed in this contribution. The new stable germanium(II) compounds **3** and **4** have been synthesized by reaction of **1** with RLi (R = Me, OMe) and fully characterized. The crystal structures of **1**−**3** and their electronic structures have been determined by X-ray diffraction and UV-photoelectron spectroscopy (UPS), respectively. DFT calculations on **1** and **3** were carried out at the B3LYP level of theory. Natural bond orbital analysis for the model molecules **1′** and **3′** (without phenyl) gives information on the Ge−Σ bonding. It turns out from the NMR, mass spectroscopy, and X-ray molecular geometry properties together with the ab initio calculations that the three-coordinated germanium(II) compound L^2GeX is best described by a model structure corresponding to a divalent germanium species weakly coordinated with the halide group, $L^2Ge^+\cdots X^-$. This view is confirmed by the particularly low energetic values of the X atom lone-pair ionizations.

Introduction

This work is part of our systematic investigation of the heavier group 14 element analogues of carbenes >M(II) (M = Ge, Sn, Pb). After our previous extensive research on thermally stable or transient germylenes,[1] we initiated, a few years ago, the synthesis and characterization of divalent compounds of germanium, tin, and lead, supported by amine-substituted phenolate[2a−c] and salen[2d−f] ligands; we recently turned to the β-diketiminato ligand framework as a promising template for stabilizing divalent M_{14} compounds. The chemistry of this family of ligand is now well-developed.[3] In our initial publication,[4a] we described the preparation, characterization, and various aspects of the chemistry of three-coordinate divalent germanium L^2GeX derivatives (X = Cl (**1**), I (**2**)) with the β-diketiminato L^2 = PhNC(Me)CHC(Me)NPh ligand.[4] Here, we present syntheses and characterizations of the new compounds L^2-GeMe (**3**) and L^2GeOMe (**4**) and, to investigate the peculiar role that this ligand and the Σ substituents play in these compounds, we analyze (i) the solid-state structures of **1**−**3** and (ii) the electronic structure of these compounds by density functional theory (DFT) (for **1** and **3**) and by UV photoelectron spectroscopy (PES) (for **1**−**3**). While this work was in progress, the preparation and the structures of a few other germylated compounds with a diketiminato ligand bearing a sterically demanding substituent at the nitrogen atoms were reported.[5]

* To whom correspondence should be addressed. E-mail: J.B., barrau@chimie.ups-tlse.fr; G.P.-G., genevieve.pfister@univ-pau.fr.
[†] Université Paul Sabatier.
[‡] Université de Pau et des Pays de l'Adour.

(1) Barrau, J.; Rima, G. *Coord. Chem. Rev* **1998**, *593*, 178 and references therein.
(2) (a) Barrau, J.; Rima, G.; El Amraoui, T. *Organometallics* **1998**, *17*, 607. (b) Barrau, J.; Rima, G.; El Amraoui, T. *J. Organomet. Chem.* **1998**, *570*, 163. (c) Barrau, J.; Rima, G.; El. Amraoui, T. *J. Organomet. Chem.* **1998**, *561*, 167. (d) Agustin, D.; Rima, G.; Gornitzka, H.; Barrau, J. *J. Organomet. Chem.* **1999**, *592*, 1. (e) Agustin, D.; Rima, G.; Gornitzka, H.; Barrau, J. *Main Group Met. Chem.* **1997**, *20*, 791. (f) Agustin, D.; Rima, G.; Gornitzka, H.; Barrau, *Eur. J. Inorg. Chem.* **2000**, 693.
(3) Bourget-Merle, L.; Lappert, M. F.; Severn, J. R. *Chem. Rev.* **2002**, *102*, 3031 and references quoted therein.
(4) (a) Akkari, A.; Byrne, J. J.; Saur, I.; Rima, G.; Gornitzka, H.; Barrau, J. *J. Organomet. Chem.* **2001**, *622*, 190. (b) Chrostowska, A.; Lemierre, V.; Pigot, T.; Pfister-Guillouzo, G. Saur, I.; Miqueu, K.; Rima, G.; Barrau, J. *Main Group Met. Chem.* **2002**, *25*, 469. (c) Saur, I.; Rima, G.; Gornitzka, H.; Miqueu, K.; Barrau, J. *Organometallics* **2003**, *22*, 1106. (d) Saur, I.; Rima, G.; Miqueu, K.; Gornitzka, H.; Barrau, J. *J. Organomet. Chem.* **2003**, *672*, 77.
(5) (a) Ayers, A. E.; Klapötke, T. M.; Dias, H. V. R. *Inorg. Chem.* **2001**, *40*, 1000. (b) Ding, Y.; Roesky, H. W.; Noltemeyer, M.; Schmidt, H. G.; Power, P. P. *Organometallics* **2001**, *20*, 1190. (c) Ding, Y.; Hao, H.; Roesky, H. W.; Noltemeyer, M.; Schmidt, H. G. *Organometallics* **2001**, *20*, 4806. (d) Ding, Y.; Ma, Q.; Roesky, H. W.; Herbst-Irmer, R.; Uson, I.; Noltemeyer, M.; Schmidt, H.-G. *Organometallics* **2002**, *21*, 5216. (e) Ding, Y.; Ma, Q.; Usön, I.; Roesky, H. W.; Noltemeyer, M.; Schmidt, H. G. *J. Am. Chem. Soc.* **2002**, *124*, 8542.

10.1021/om030154y CCC: $25.00
Publication on Web 06/27/2003

Scheme 1

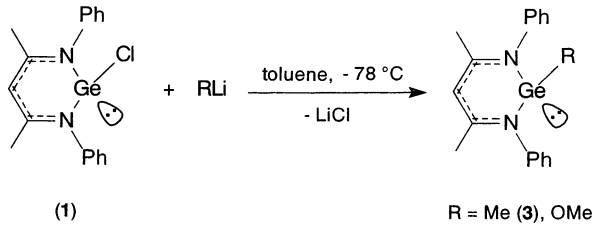

Table 1. Selected ^{1}H and ^{13}C{^{1}H} NMR (C_6D_6) Data for 1−4

	L^2H[a]	**1**[a]	**2**[a]	**3**	**4**
		^{1}H NMR (δ, ppm)			
CH	4.77	5.07 (5.39)[b]	5.23 (5.64)[b]	4.78	4.84
Me	1.80	1.61 (1.96)[b]	1.56 (2.05)[b]	1.63	1.69
		^{13}C NMR (δ, ppm)			
CH	98.14	102.1	103.9	98.49	101.5
Me	20.77	23.75	23.49	20.84	23.12

[a] Reference 4a. [b] δ in $CDCl_3$.

Results and Discussion

1. Synthesis of Compounds 3 and 4 and Structures of 1−3. Compounds **3** and **4** were isolated as orange-red crystalline solids in high yields (75−90%) from the metathesis reactions of **1** with 1 equiv of MeLi or MeOLi in toluene (Scheme 1) and were fully characterized by elemental analysis, EI-MS, and multinuclear NMR spectroscopy.

The divalent germanium species **3** and **4** are soluble in aromatic and polar solvents and are stable under an inert atmosphere for a long time, while the halide analogues **1** and **2** show a lower solubility (specially **2**) in aromatic solvents, perhaps as a result of a more ionic structure.

The ^{1}H and ^{13}C NMR spectra of **3** and **4** were consistent with their formula. Both ^{1}H and ^{13}C NMR data corresponding to the L^2 unit are very similar for **1**−**4** (Table 1). As in the case of the free ligand, the equivalence of methyl and phenyl groups indicates the presence of C_s symmetry in solution for **3** and **4**. ^{1}H NMR resonances of the methine and methyl ring of **1**−**4** (Table 1) show a downfield and an upfield shift, respectively, relative to those of L^2H. ^{13}C NMR chemical shifts are also different, the methine and methyl carbons being downfield for **1**−**4** compared to those corresponding to the L^2H free ligand (Table 1). It is noteworthy that the resonances of the methine proton and carbon in ^{1}H and ^{13}C NMR of L^2GeMe (δ(^{1}H) 4.78 ppm; δ(^{13}C) 98.49 ppm) show an upfield shift compared to the corresponding resonances of L^2GeOMe (δ(^{1}H) 4.84 ppm; δ(^{13}C) 101.5 ppm) and a much more upfield shift compared to those of L^2GeCl (δ(^{1}H) 5.07 ppm; δ(^{13}C) 102.1 ppm). For L^2GeI, the chemical shifts are downfield (δ(^{1}H) 5.23 ppm; δ(^{13}C) 103.9 ppm) compared to those in **1**, **3**, and **4**; this may be the result of an increased positive charge at the germanium (or on the ligand backbone) due to a weakly coordinated iodide anion. The chemical shifts for **1** and **2** vary strongly with the solvent; polar solvents lead to strong deshielding, probably as a result of a solvent-dependent polarization of the Ge···X contact (Table 1).

The mass spectra of **1**−**4** show in all cases that the base peak corresponds to $[L^2Ge]^+$. The molecular ion $M^{\bullet+}$ peaks of compounds **1**, **3**, and **4** are detected with intensities of 45, 9, and 13% of the $[L^2Ge]^+$ base peaks, respectively, indicating the relative stabilities of these molecular ions in the gas phase. The low degree of ion pairing in **2** $[L^2Ge]^+\cdots I^-$ is revealed in the gas phase by the absence of the molecular ion $M^{\bullet+}$ peak in the mass spectrum (EI), the larger and more prominent peak corresponding in this case to $[L^2Ge]^+$. It is noteworthy that this cationic L^2Ge^+ species[4a] and the comparable cationic aminotroponiminate [(*i*Pr$_2$)ATI]-Ge^+ [6] have been isolated, which confirms the high stability of such cationic derivatives of germanium(II) with supporting polydentate ligands.

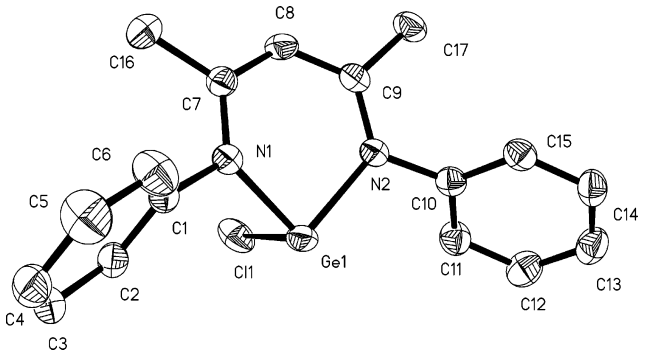

Figure 1. Solid-state structure of $L^2Ge(Cl)$ (**1**) (ellipsoids are drawn at the 50% probability level). Hydrogen atoms are omitted for clarity. Selected bond lengths (Å) and bond angles (deg): Ge−N(1) = 1.955(2), Ge−N(2) = 1.965(1), Ge−Cl = 2.340(6), N(2)−C(9) = 1.337(2), N(1)−C(7) = 1.338(2), C(9)−C(8) = 1.390(2), C(8)−C(7) = 1.391(2); N(1)−Ge−N(2) = 90.28(6), N(1)−Ge−Cl = 93.55(5), N(2)−Ge−Cl = 94.95(4).

The structures of compounds **1**−**3** were determined by single-crystal X-ray diffraction. Crystals of **1** and **2** (yellow) and **3** (red) suitable for single-crystral analysis were obtained from a toluene solution at −30 °C within 3 days. The solid-state structures are shown in Figures 1−3. Crystallographic data and processing parameters are given in Table 2. The X-ray single-crystal figures of **1**−**3** display the monomeric structures of all compounds. The structure of **1** was briefly reported in a preliminary account,[4b] and the structural features of the iodo (**2**) and methyl (**3**) congeners are quite similar. In all these divalent species, the germanium center is at the apex of a distorted trigonal pyramid. Perusal of the germanium−ligand atom distances suggests that the ligand is essentially symmetrically bound to the germanium in **1**−**3**. The five ligand atoms are almost coplanar, the planarity being confirmed by the fact that the sums of the internal angles for the six-membered L^2Ge rings are 713° (**1**), 717° (**2**), and 708° (**3**), respectively. The side views of the three compounds (Figure 4) show that the iodo germylene **2** has the most planar C_3N_2 ring (x = 0.04 Å; y = 0.35 Å), whereas the methylgermylene **3** has the greatest deviation from planarity (x = 0.15 Å; y = 0.62 Å). Due to their steric hindrance, the two phenyl rings are found almost orthogonal to the C_3N_2 plane in **1**−**3**. In all these compounds, the average Ge−N bonds (1.955−2.022 Å) are between N−Ge donor−acceptor bonds (2.050−2.110 Å)[5a,7] and covalent N−Ge^{II} bonds (1.870−1.890 Å).[5a,8] The Ge−N bond lengths of L^2GeMe (2.010(4), 2.022(4) Å) are longer than those in L^2GeX

(6) Dias, R. H. V.; Wang, Z. *J. Am. Chem. Soc.* **1997**, *117*, 44650.

Table 2. Crystal Data and Structure Refinement Details for 1,[a] 2, and 3

	1	2	3
empirical formula	$C_{17}H_{17}ClGeN_2$	$C_{17}H_{17}GeIN_2$	$C_{18}H_{20}GeN_2$
fw	357.37	448.82	336.95
cryst syst	orthorhombic	orthorhombic	triclinic
space group	$P2_12_12_1$	$P2_12_12_1$	$P\bar{1}$
a (Å)	8.8117(5)	7.283(1)	7.371(2)
b (Å)	13.5830(8)	8.805(1)	9.173(3)
c (Å)	13.8910(8)	26.107(3)	13.049(4)
β (deg)	-	-	82.716(6)
V (Å^3)	1662.60(17)	1674.2(3)	827.5(4)
Z	4	4	2
calcd density (Mg/m^3)	1.428	1.781	1.352
abs coeff (mm^{-1})	1.998	3.669	1.846
cryst size (mm)	0.3 × 0.4 × 0.5	0.1 × 0.2 × 0.5	0.1 × 0.2 × 0.6
θ range for data (deg)	2.10−29.45	1.56−26.37	1.66−24.11
no. of rflns	11 373	9788	3950
no. of indep rflns	4266 (R_{int} = 0.0198)	3409 (R_{int} = 0.0514)	2593 (R_{int} = 0.0455)
abs cor	semiempirical	semiempirical	semiempirical
min/max transmission	0.6641	0.5489	0.6643
no. of params	192	192	193
goodness of fit on F^2	1.048	0.996	1.005
R1[b] ($I > 2\sigma(I)$)	0.0219	0.0327	0.0521
wR2[c] (all data)	0.0508	0.0763	0.1412
largest diff peak, hole (e Å^{-3})	0.352, −0.184	0.817, −0.778	1.227, −0.872

[a] Reference 4b. [b] $R1 = \sum||F_o| - |F_c||/\sum|F_o|$. [c] $wR2 = \{\sum[w(F_o^2 - F_c^2)^2]/\sum[w(F_o^2)^2]\}^{1/2}$.

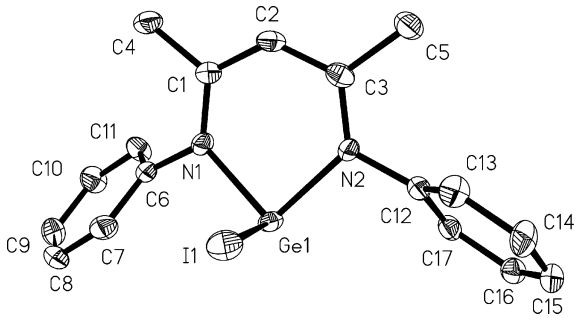

Figure 2. Solid-state structure of L^{2}Ge(I) (**2**) (ellipsoids are drawn at the 50% probability level). Hydrogen atoms are omitted for clarity. Selected bond lengths (Å) and bond angles (deg): Ge−N(1) = 1.971(4), Ge−N(2) = 1.959(4), Ge−I = 2.778(6), N(1)−C(1) = 1.345(6), N(2)−C(3) = 1.351(6), C(1)−C(2) = 1.391(7), C(2)−C(3) = 1.397(7); N(1)−Ge−N(2) = 91.83(17), N(1)−Ge−I = 98.37(12), N(2)−Ge−I = 92.98(12).

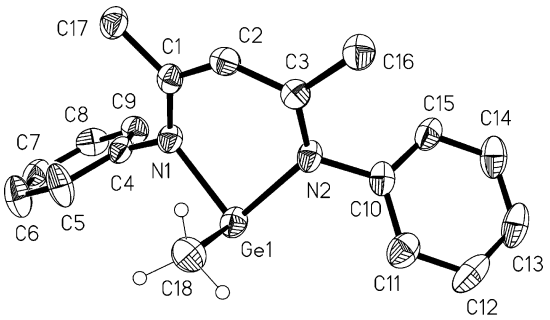

Figure 3. Solid-state structure of L^{2}Ge(Me) (**3**) (ellipsoids are drawn at the 50% probability level). Hydrogen atoms are omitted for clarity. Selected bond lengths (Å) and bond angles (deg): Ge−N(1) = 2.022(4), Ge−N(2) = 2.010(4), Ge−C(18) = 2.014(6), N(1)−C(1) = 1.332(6), N(2)−C(3) = 1.350(6), C(1)−C(2) = 1.411(6), C(2)−C(3) = 1.395(7); N(1)−Ge−N(2) = 88.81(15), N(1)−Ge−C(18) = 94.1(2), N(2)−Ge−C(18) = 96.08(2).

(X = I, 1.959(4), 1.971(4) Å; X = Cl, 1.955(2), 1.965(1) Å); this is probably due to the different inductive effects of the various substituents. Interestingly for L^{2}GeMe, although the Ge−N(1) and the Ge−N(2) distances are identical, the N(1)−C(1) and C(2)−C(3) distances are slightly shorter than N(2)−C(3) and C(1)−C(2), respectively, indicating an alternating, more localized distribution of electrons in the ligand than for L^{2}GeCl and L^{2}GeI. The N(1)−Ge−N(2) bond angles for **1**−**3** are close to 90°; this angle increases from L^{2}GeMe (88.8°) to L^2-GeCl (90.3°) and L^{2}GeI (91.8°), and these variations are the result of both electronic and steric effects of the Σ substituents. For the previously described L′^{2}GeCl compounds (L′^{2} = ArNC(Me)CHC(Me)NAr; Ar = 2,6-*i*-Pr$_2$C$_6$H$_3$)[5b] a lengthening of the Ge−N bonds (1.99, 1.99 Å) is observed compared to those in L^{2}GeCl; these bond elongations can be attributed to the increased steric demand of the bulky aryl groups of the β-diketiminato ligand in these compounds. The Ge−C distance in **3** (2.014(6) Å) is in the normal range for divalent compounds (Ge−C = 1.989−2.067 Å),[9a−c] while the Ge−X lengths in **1** and **2** (**1**, 2.340(6) Å; **2**, 2.778(6) Å) are

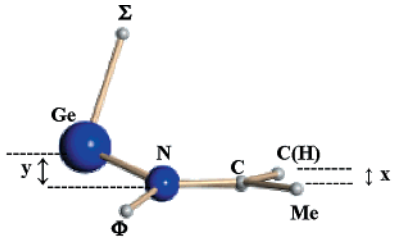

Experimental and calculated (in parentheses) values of the distances of C(H) and Ge from the C_3N_2 plane (x and y, respectively).

Compounds	1	2	3
x (Å)	0.09 (0.112)	0.04	0.15 (0.152)
y (Å)	0.48 (0.518)	0.35	0.62 (0.443)

Figure 4. Side view of **1**−**3**: R = Cl (**1**), I (**2**), Me (**3**).

(7) (a) Schmidt, H.; Keitemeyer, S.; Neumann, B.; Stammler, H. G.; Schoeller, W. W.; Jutzi, P. *Organometallics* **1998**, *17*, 2149. (b) Veith, M.; Becker, S.; Huch, V. *Angew. Chem., Int. Ed. Engl.* **1989**, *28*, 1237. (c) Veith, M.; Becker, S.; Huch, V. *Angew. Chem., Int. Ed. Engl.* **1990**, *20*, 216.

(8) (a) Chorley, R. W.; Hitchkock, P. B.; Lappert, M. F.; Leung, W. P.; Power, P. P.; Olmstead, M. M. *Inorg. Chim. Acta* **1992**, *198*−*200*, 203. (b) Veith, M.; Hobein, P.; Rösler, R. *Z. Naturforsch.* **1989**, 1067.

Table 3. Calculated (B3LYP/6-311G(d,p)) Geometrical Parameters (Distances in Å and Angles in deg) for L²GeCl (1) and L²GeMe (2)

	L²GeCl (**1**)[a]	L²GeMe (**3**)
Ge−N	2.03, 2.03	2.07, 2.07
Ge−Σ	2.36	2.04
N−C	1.33, 1.33	1.33, 1.33
C−C	1.40, 1.40	1.41, 1.41
N(1)−Ge−N(2)	89.4	89.0
N−Ge−Σ	94.9, 94.8	93.9, 93.8

[a] Reference 4b.

normal for three-coordinated germanium(II) compounds.[5a,9d−f] These last values are ∼10% longer than the average of previously observed Ge−X distances in various dicoordinated germanium(II) and germanium(IV) compounds (Ge−Cl = 2.11−2.20 Å; Ge−I = 2.50−2.55 Å);[9g−k] this impressive margin reflects mainly the change in coordination at the germanium and probably also a halide bonded medium-strongly to the germanium center: $L^2Ge^+\cdots X^-$.

2. UV−Photoelectron Spectroscopy Studies with Density Functional Theory Support. For a better understanding of the electronic structure and effect of the substituents Σ at the germanium of such compounds, we were particularly interested in (i) experimental UV-photoelectron spectroscopy of **1**−**3** and (ii) in NBO population and total atomic charge analyses of **1** and **3**. In a preliminay paper,[4b] we briefly described the electronic (UV-photoelectron and DFT calculations) and the molecular (X-ray crystallography) structures of L²H and L²GeCl; consequently, the experimental and theoretical studies are extended here to the iodo- and methyl-substituted species **2** and **3**, respectively.

Table 3 shows calculated geometrical parameters for L²GeMe (**3**) and, for comparison, those of L²GeCl (**1**). These calculated parameters agree well with the available X-ray experimental data (Figures 1 and 3). For **1** and **3** the calculations predict that the five ligand atoms are quasi planar, the germanium and the C(H) atoms being above the C_3N_2 plane (Figure 4) as denoted by the X-ray structure; the electronic delocalization within the ligand is also theoretically found. The two calculated σ_{Ge-N} bonds are found to be identical but slightly longer (as the Ge−Σ bonds) than the experimental X-ray values obtained for **1** and **3** (Table 3 and Figures 1 and 3).

The Becke3LYP method reproduces properly the experimentally characterized molecular structures of both **1** and **3**; we used this theoretical description for assignments of the experimental IP recorded by He I and He II photoelectron spectroscopy for **1**−**3**.

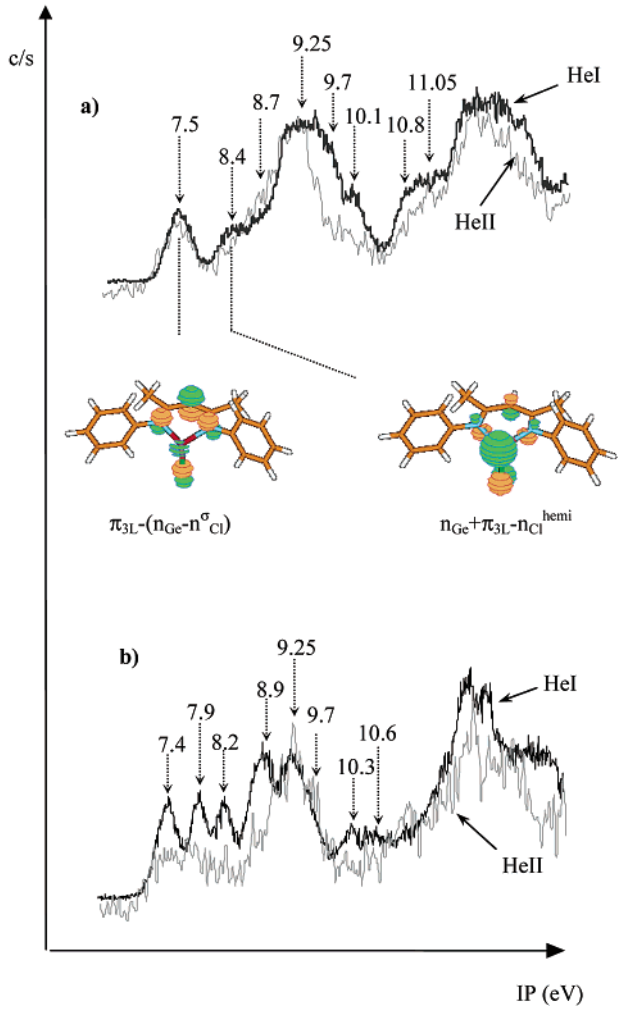

Figure 5. He I and He II photoelectron spectra (IP in eV): (a) L²Ge(Cl) (**1**) and Molden[25] visualization of the two first molecular orbitals; (b) L²Ge(I) (**2**).

The He I and He II photoelectron spectra of L²GeI (Table 4, Figure 5b) display three well-resolved bands at 7.4, 7.9, and 8.2 eV, followed by one band at 8.9 eV and a broader one centered at 9.25 eV with a shoulder at 9.7 eV. Other less intense bands appear at higher energies (10.3, 10.6 eV). The two first ionization potentials at 7.4 and at 7.9 eV (Figure 5b) correspond, as for the chlorine derivative (Table 4, Figure 5a), to the molecular orbitals having a strong participation of the germanium and iodine lone pairs in interaction with the $\pi(\pi_{3L})$ orbital of the ligand. This assignment is confirmed by the decrease of the intensity of the IP using He II

Table 4. Experimental Ionization Potentials and KS Energies (in eV) and the Nature of Molecular Orbitals for L²GeCl (1) and L²GeI (2)

KS L²GeCl (**1**)[a] calcd[b]	nature of MO	IP L²GeCl (**1**)[a] exptl	IP L²GeI (**2**) exptl	nature of MO
−5.94	$\pi_{3L} - (n_{Ge} - n^{\sigma}_{Cl})$	7.5	7.4	$\pi_{3L} - (n_{Ge} - n^{\sigma}_{I})$
−6.38	$n_{Ge} + \pi_{3L} - n_{Cl}^{hemi}$	8.4	7.9	$n_{Ge} + \pi_{3L} - n_{I}^{hemi}$
−6.87	$\varphi^- b_1$	8.7	8.2	$n_{I}^{peri} - \varphi^- a_2$
			8.9	n_{I}^{hemi}
−7.17; −7.18; −7.24	$\varphi^+ b_1$; $\varphi^- a_2 - n_{Cl}^{peri}$; $\varphi^+ a_2$	9.25	9.25	$\varphi^- b_1$; $\varphi^+ b_1$; $\varphi^+ a_2$; $\varphi^- a_2$
−7.34; −7.46	n_{Cl}^{peri}; n_{Cl}^{hemi}	9.7	9.7 sh	π_{2L}
−8.57	π_{2L}	10.15		
−9.02	$\sigma^+_{GeN} - \sigma_{GeCl}$	10.8	10.3	$\sigma^+_{Ge-N} - \sigma_{Ge-I}$
−9.16	σ^-_{GeN}	11.05	10.6	σ^-_{GeN}

[a] Reference 4b. [b] ΔSCF =7.43 eV; see the Experimental Section.

Table 5. Experimental Ionization Potentials and KS Energies (in eV) and the Nature of Molecular Orbitals for L^2GeMe (3)

L^2GeMe (**3**) calcd[a] KS	nature of MO	L^2GeMe (**3**) exptl IP
−4.89	$n_{Ge} - \sigma_{CH_3} - \pi_{3L}$	6.7
−5.97	$\pi_{3L} + n_{Ge}$	7.7
−6.67	$\varphi^- b_1$	8.5
−6.94; −7.11; −7.12	$\varphi^+ b_1; \varphi^- a_2; \varphi^+ a_2$	9.1
−8.16	$\sigma^+_{GeN} - \sigma_{GeCH_3}$	9.7
−8.23	π_{2L}	
−8.71	σ^-_{GeN}	10.5

[a] ΔSCF= 6.48 eV; see the Experimental Section.

radiation. The significant decrease in the intensity of the two bands corresponding to the higher energies 8.2 and 8.9 eV, on He II radiation, is also unambiguously indicative of the participation of the iodine lone pair orbitals. The band at 9.25 eV is associated with ejection of electrons of the phenyl substituent (orthogonal substituent). The shoulder at 9.7 eV and the ionizations at 10.3 and 10.6 eV can be attributed to the π_{2L} (π_{CN} antisymmetric combination), σ^+_{GeN} (with iodine participation), and σ^-_{GeN} orbitals ionizations, respectively. Concerning the ionizations of the lone pairs on the halogen atoms, it is noteworthy that lower energies are needed for L^2GeCl (9.7 eV (n_{Cl})) and L^2GeI (8.9, 8.2 eV-(n_I)) (Table 4) than for the corresponding dihalogermanium(II) compounds GeX_2[10,11] ($GeCl_2$, 12.69 (a_1, σ^+_{Cl}), 12.58 (b_2, π^+_{Cl}), 11.70 (a_2, π^-_{Cl}), 11.44 (b_1, σ^-_{Cl}), average 12.10 eV; GeI_2, 10.62 (a_1, σ^+_I), 10.62 (b_2, π^+_I), 9.83 (a_2, π^-_I), 9.50 (b_1, σ^-_I), average 10.14 eV). This is indicative of more highly charged halogen atoms in compounds **1** and **2** than in dihalides GeX_2.

Replacement of a halogen atom by a methyl group causes a decrease in IP values. Table 5 lists Kohn−Shan energies and corresponding experimental values. The spectrum of **3** (Figure 6) displays four resolved bands followed by a broad signal. On the basis of calculations, the two bands at low energies (6.7 and 7.7 eV) are assigned to the ionizations of the germanium lone pair in combination with the ligand π system (6.7 eV, $n_{Ge} - \sigma_{CH_3} - \pi_{3L}$; 7.7 eV, $\pi_{3L} + n_{Ge}$). It is noteworthy that, in contrast to that observed for the chlorine derivative **1**, the participation of the germanium lone pair (n_{Ge}) and of the (π_{3L}) ligand are prominent, in the associated molecular orbitals, respectively. The bands at 8.5 and 9.1 eV are associated with the ionizations of the phenyl groups. The broad massif at 9.7−10.5 eV corresponds to three ionizations: two originating from the σ_{Ge-N} bonds and the other from the π_{2L} system of the ligand.

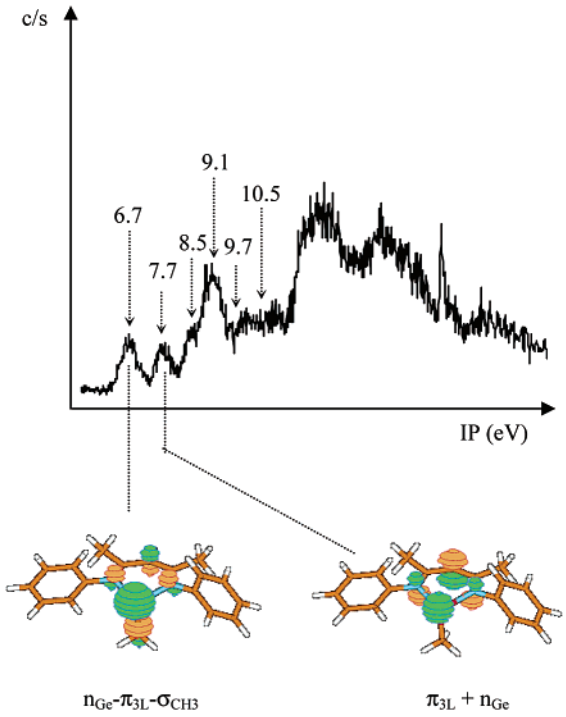

Figure 6. He I photoelectron spectrum of $L^2Ge(Me)$ (**3**) (IP in eV) and Molden[25] visualization of the first two molecular orbitals.

It is noteworthy that we were unable to record an intense He II spectrum of **3**.

Natural bond orbital[12] analysis for the model (without phenyl substituents) molecules **1′** and **3′** gives information on the Ge−Σ bonding. It confirms that the contribution (80%) of the chlorine is higher than that of the CH_3 moiety (72%) to form the Ge−Σ bonds. The ligand backbone does not form a perfectly planar system; accordingly, it is difficult to estimate the electron density distribution in the π orbitals but the analysis of the p_π natural bond orbital population denotes an electron density loss of 0.2 and 0.1 e for **1′** and **3′**, respectively, indicating a donation to the germanium atom.

Considering the total atomic charges (Table 6) for **1** and **3**, it appears that the substituent at the germanium is negatively charged, depending on the nucleophilicity of Σ. The comparison with the chlorine charges found for $GeCl_2$ (−0.266) shows in the case of the compound **1** a more important chlorine atom charge (−0.474); these results are in accord with the experimental IPs (vide supra). Moreover, the total charges of the ligand are in good agreement with the NMR data, in particular considering the chemical shift of the methine proton C(H); the C(H) atom, being highly involved in the π homo orbital of the $L^2GeΣ$ species, is very sensitive to the electron delocalization on the germanium atom (particularly in **1** and **2**).

Conclusion

All these data suggest that a L^2GeX (X = halide) compound is better described as a N_2Ge divalent ger-

(9) (a) Al-Juaid, S. S.; Avent, A. G.; Eaborn, C.; Hill, M. S.; Hitchcock, P. B.; Patel, D. J.; Smith, J. D. *Organometallics* **2001**, 20, 1223. (b) Jutzi, P.; Becker, A.; Stammler, H. G.; Neumann, B. *Organometallics* **1997**, *10*, 1647. (c) Jutzi, P.; Keitemeter, S.; Neumann, B.; Stammler, H. G. *Organometallics* **1999**, *18*, 4778. (d) Jutzi, P.; Keitemeyer, S.; Neumann, B.; Stammler, A.; Stammler, H. G. *Organometallics* **2001**, *20*, 42. (e) Inoguchi, Y.; Okui, S.; Mochida, K.; Itai, A. *Bull. Chem. Soc. Jpn.* **1985**, *58*, 974. (f) Stobart, S. R.; Churchill, M. R.; Hollander, F. J.; Youngs, W. J. *J. Chem. Soc., Chem. Commun.* **1979**, 911. (g) Moreno, Y.; Nakamura, Y.; Iijima, T. *J. Chem. Phys.* **1960**, *32*, 643. (h) Drake, J. E.; Hencher, J. L.; Shen, Q. *Can. J. Chem.* **1977**, *55*, 1104. (i) Walz, L.; Thiery, D.; Peters, E. M.; Wendel, H.; Schönher, E.; Wojnowski, M. *Z. Kristallogr.* **1993**, *208*, 207. (j) Filipou, A. C.; Portius, P.; Philippopoulos, A. I. *Organometallics* **2002**, *21*, 653. (k) Pu, L.; Olmstead, M. M.; Power, P. P.; Schiemenz, B. *Organometallics* **1998**, *17*, 5602.
(10) Jonkers, G.; Van der Kerk, S. M.; De Lange, C. A. *Chem. Phys.* **1982**, *70*, 69.
(11) Jonkers, G.; Van der Kerk, S. M.; Mooyman, R.; De Lange, C. A.; Snijders, J. G. *Chem. Phys. Lett.* **1983**, *94*, 585.
(12) (a) Reed, A. E.; Curtiss, L. A.; Weinhold, F. *Chem. Rev.* **1988**, *88*, 899. (b) Foster, J. P.; Weinhold, F. *J. Am. Chem. Soc.* **1980**, *102*, 7211.

Table 6. Calculated (B3LYP/6-311G(d,p)) Total Atomic Charges (Mulliken) for L²GeCl (1) and L²GeMe (3)

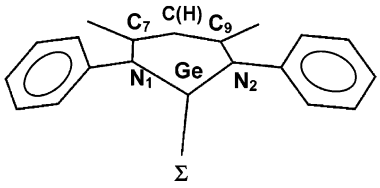

	total charge			total charge	
atom	Σ = Cl	Σ = Me	atom	Σ = Cl	Σ = Me
Ge	0.655	0.617	Σ	−0.474	−0.284
N_1	−0.615	−0.607	$Ph(N_1)$	0.196	0.157
N_2	−0.621	−0.609	$Ph(N_2)$	0.197	0.157
C_7	0.269	0.250	$Me(C_7)$	0.120	0.109
C(H)	−0.203	−0.232	$Me(C_9)$	0.120	0.110
C_9	0.268	0.248	$H(C_8)$	0.090	0.083

manium more or less coordinated with an halide group, $N_2Ge^+\cdots X^-$, than a $XGe^+\cdots N_2^-$ species, as postulated in our preliminary report. Suggestion of such a qualitative model for these three-coordinate germanium(II) species is more particularly supported by the following observations: (i) the downfield chemical shift of the C(H) ring proton, which varies strongly with the nature of X and presents a solvatochromic behavior, (ii) the long Ge−X distances, (iii) the low ionization potentials of the halogen lone pairs, which indicate particularly charged atoms, and (iv) the presence of the molecular $[L^2Ge]^+$ ion in the gas phase, which proves its high stability. In this model the anion/cation separation and thus eventual delocalization of the positive charge on the L^2Ge ring depends on the nature of X. Moreover, though the π electrons of the L^2Ge ring system appear to be mostly delocalized on nitrogen and carbon atoms, it seems possible to assume a weak π ligand $\rightarrow \sigma^*_{Ge-X}$ interaction (negative hyperconjugation), permitting a ligand-to-germanium transfer of π-electron density. A further extension of this study to other group 14 elements, β-diketiminate, and X ligands is now in progress in order to specify the electronic organization in these species.

Experimental Section

General Procedures. All manipulations were carried out under an argon atmosphere with the use of standard Schlenk and high-vacuum-line techniques. Solvents were distilled from conventional drying agents and degassed twice prior to use.[13] ^{1}H NMR spectra were recorded on a Bruker AC 80 spectrometer operating at 80 MHz (chemical shifts are given in ppm (δ) relative to Me_4Si) and ^{13}C spectra on a AC-200 MHz spectrometer operating at 62.9 MHz; the multiplicity of the ^{13}C NMR signals was determined by the APT technique. Mass spectra were recorded on a Nermag R10-10H or a Hewlett-Packard 5989 instrument operating in the electron impact mode at 70 eV, and samples were contained in glass capillaries under argon. IR spectra were obtained on a Perkin-Elmer 1600 FT-IR. Irradiations were carried out at 25 °C by using a low-pressure mercury immersion lamp in a quartz tube. Melting points were taken on a hot-plate microscope apparatus from Leitz Biomed. Elemental analyses (C, H, N) were performed at the Microanalysis Laboratory of the Ecole Nationale Supérieure de Chimie de Toulouse.

Synthesis of L²GeMe (3). A solution of MeLi (0.42 mL, 1.6 M in ether) was added to a stirred solution of **1** (0.24 g, 0.67 mmol) in toluene (25 mL) at −78 °C. The reaction mixture was warmed to room temperature and stirred for 2 h. Filtration and storage of the remaining solution in a −30 °C freezer for 3 days afforded orange-red crystals of **3** (0.19 g, 83%). **3**: mp 80−84 °C. ^{1}H NMR (C_6D_6): δ 0.74 (s, 3H, CH_3), 1.63 (s, 6H, $2CH_3$), 4.78 (s, 1H, CH), 6.88−7.10 (m, 10H, C_6H_5). ^{13}C NMR (C_6D_6): δ 11.88 (CH_3), 20.84 ($2CH_3$), 98.49 (CH), 125.81 (*m* aryl C), 126.87 (*p* aryl C), 128.46 (*o* aryl C), 147.00 (C_{quat}), 163.26 (C−N). MS: *m*/*z* 338 $[M]^{\bullet+}$. Anal. Calcd for $C_{18}H_{20}N_2Ge$: C, 64.16; H, 5.98; N, 8.31. Found: C, 64.37; H, 5.90; N, 7.92.

Synthesis of L²GeOMe (4). A solution of **1** (0.24 g, 0.66 mmol) in toluene (15 mL) was added dropwise to a stirred suspension of MeOLi (0.25 g, 0.66 mmol) in toluene (15 mL) at −78 °C. The reaction mixture was warmed to room temperature and stirred for 2 h. The precipitate was filtered off, and the solvent of the resulting solution was removed under vacuum to yield **4** as an orange-red solid (0.2 g, 87%). **4**: mp 81−85 °C. ^{1}H NMR (C_6D_6): δ 1.69 (s, 6H, $2CH_3$), 3.92 (s, 3H, OCH_3), 4.84 (s, 1H, CH), 6.84−7.13 (m, 10H, C_6H_5). ^{13}C NMR (C_6D_6): δ 23.12 (CH_3), 52.75 (OCH_3), 101.48 (CH), 125.81 (*m* aryl C), 126.87 (*p* aryl C), 128.46 (*o* aryl C), 146.37 (C_{quat}), 163.47 (C−N). MS: *m*/*z* 354 $[M]^{\bullet+}$. Anal. Calcd for $C_{18}H_{20}N_2OGe$: C, 61.25; H, 5.71; N, 7.94. Found: C, 61.64; H, 5.85; N, 7.80.

UV-Photoelectron Spectroscopy. Photoelectron spectra were recorded on an Helectros 0018 spectrometer and monitored by a microcomputer system supplemented by a D-A converter. The spectra contain 2000 points and are accurate to 0.1 eV. They were recorded with 21.21 eV He I and 40.81 eV He II irradiation as a photon source and calibrated on the well-known helium autoionization at 4.98 eV and nitrogen autoionizations at 15.59 and 16.98 eV. It is worth mentioning that, on going from He I to He II ionization energies, the bands arising from ejection of an electron from an orbital localized on second or third row decrease in intensity. These relative intensity changes are attributed to variations in the one- and two-center contributions to the photoionization cross-sections of the corresponding molecular orbitals.[14]

Computational Methods. The calculations were performed using the Gaussian 98 program package.[15] The optimization and vibrational analyses were carried out with density functional theory (DFT) using the B3LYP[16] functional in conjunction with a 6-311G(d,p) basis set.

The influence of the basis[17] set chosen on the KS energy levels being important, we applied the 6-311G basis set for calculations on **1** and **3**, but we could not do the same for **2** because no 6-311G basis is available for iodine.

(13) Perrin, D. D.; Armarego, W. L. F.; Perrin, D. R. *Purification of Laboratory Chemicals*; Pergamon Press: New York, 1985.

(14) (a) Schweig, A.; Thiel, W. *J. Electron Spectrosc. Relat. Phenom.* **1974**, *3*, 27. (b) Schweig, A.; Thiel, W. *Mol. Phys.* **1974**, *27*, 265.

(15) Frisch, M. J.; Trucks, G. W.; Schlegel, H. B.; Scuseria, G. E.; Robb, M. A.; Cheeseman, J. R.; Zakrzewski, V. G.; Montgomery, J. A., Jr.; Stratmann, R. E.; Burant, J. C.; Dapprich, S.; Millam, J. M.; Daniels, A. D.; Kudin, K. N.; Strain, M. C.; Farkas, O.; Tomasi, J.; Barone, V.; Cossi, M.; Cammi, R.; Mennucci, B.; Pomelli, C.; Adamo, C.; Clifford, S.; Ochterski, J.; Petersson, G. A.; Ayala, P. Y.; Cui, Q.; Morokuma, K.; Malick, D. K.; Rabuck, A. D.; Raghavachari, K.; Foresman, J. B.; Cioslowski, J.; Ortiz, J. V.; Stefanov, B. B.; Liu, G.; Liashenko, A.; Piskorz, P.; Komaromi, I.; Gomperts, R.; Martin, R. L.; Fox, D. J.; Keith, T.; Al-Laham, M. A.; Peng, C. Y.; Nanayakkara, A.; Gonzalez, C.; Challacombe, M.; Gill, P. M. W.; Johnson, B. G.; Chen, W.; Wong, M. W.; Andres, J. L.; Head-Gordon, M.; Replogle, E. S.; Pople, J. A. *Gaussian 98*, revision A.7; Gaussian, Inc.: Pittsburgh, PA, 1998.

(16) (a) Parr, R. G.; Yang, W. *Functional Theory of Atoms and Molecules*; Oxford University Press: New York, 1989. (b) Becke, A. D. *Phys. Rev.* **1988**, *38*, 3098. (c) Becke, A. D. *J. Chem. Phys.* **1993**, *98*, 5648. (d) Lee, C.; Yang, W.; Parr, R. G. *Phys. Rev.* **1988**, *B37*, 785.

(17) (a) Joantéguy, S.; Pfister-Guillouzo, G.; Chermette, H. *J. Phys. Chem.* **1999**, *103*, 3505. (b) Frish, M. J.; Trucks, G. W.; Cheeseman, J. R. Systematic Model Chemistries Based on Density Functional Theory: Comparison with Traditional Models and with Experiment. In *Recent Development and Applications of Modern Density Functional Theory, Theoretical and Computational Chemistry*; Semminario, J. M., Ed.; Elsevier Science: Amsterdam, 1996; Vol. 4, pp 679−707.

Recent works[18−21] have shown that ϵ_i^{KS} can be linked to experimental vertical ionization potentials (IP_v) by the uniform shift x. The value of x is taken as $x = |-\epsilon_i(HOMO) - IP_v^{exptl}|$. This approach gives a good agreement with experimental values and is justified by the fact that the first calculated vertical ionization potential IP_v^{calcd} (as the difference E_T(cation) − E_T(neutral molecule)) lies very close to experimental values. Stowasser and Hoffman[22] have recently shown that the localizations of KS orbitals are very similar to those obtained after HF calculations. Thus, it is possible to determine the nature of the first ionizations and to interpret the photoelectron spectra unambiguously.

ΔSCF is the first vertical ionization potential IP_{1v}^{calcd}, which is calculated as the difference E_T(cation) − E_T(neutral molecule).

X-ray Crystal Structure Determination of Compounds 1−3. Suitable yellow (**1**, **2**) and red (**3**) crystals for X-ray diffraction experiments were obtained at low temperature (−20 °C) by cooling concentrated toluene solutions of **1**−**3**. Crystal data for **1**−**3** are presented in Table 2. All data were collected at low temperatures on a Bruker-AXS CCD 1000 diffractometer with Mo Kα radiation ($\lambda = 0.710\ 73$ Å). The structures were solved by direct methods by means of SHELXS-97[23] and refined with all data on F^2 by means of SHELXL-97.[24] All non-hydrogen atoms were refined anisotropically. The hydrogen atoms of the molecules were geometrically idealized and refined using a riding model. Full details of the crystallographic analysis of **2** and **3** are given in the Supporting Information.

Acknowledgment. We thank the IDRIS (CNRS, Orsay, France) for calculation facilities and P. Baylere for technical assistance.

Supporting Information Available: Tables giving crystallographic data and structure refinement details, atomic coordinates and displacement parameters, and bond lengths and angles for the crystal structures of compound **2** and **3** and calculation files (**Z** matrix, repulsion, and total energies: ZPE correction) for **1** and **3**. This material is available free of charge via the Internet at http://pubs.acs.org.

OM030154Y

(18) Arduengo, A. J.; Bock, H.; Chen, H.; Denk, M.; Dixon, D. A.; Green, J. C.; Hermann, W. A.; Jones, N. L.; Wagner, M.; West, R. *J. Am. Chem. Soc.* **1994**, *116*, 6641.

(19) (a) Muchall, H.; Werstiuk, N.; Pitters, J.; Workentin, M. *Tetrahedron* **1999**, *55*, 3767. (b) Muchall, H.; Werstiuk, N.; Choudury, B.; Ma, J.; Warkentin, J.; Pezacki, J. *Can. J. Chem.* **1998**, *76*, 238. (c) Muchall, H.; Werstiuk, N.; Choudury, B. *Can. J. Chem.* **1998**, *76*, 221.

(20) Muchall, H.; Rademacher, P. *J. Mol. Struct.* **1998**, *471*, 189.

(21) Miqueu, K.; Sotiropoulos, J.-M.; Pfister-Guillouzo, G.; Ranaivonjatovo, H.; Escudié, J. *J. Mol. Struct.* **2001**, *545*, 139.

(22) Stowasser, R.; Hoffmann, R. *J. Am. Chem. Soc.* **1999**, *121*, 3414.

(23) Sheldrick, G. M. *Acta Crystallogr., Sect. A* **1990**, *46*, 467.

(24) Sheldrick, G. M. SHELXL-97, Program for Crystal Structure Refinement; Universität Göttingen, Göttingen, Germany, 1997.

(25) Schaftenaar, G.; Noordik, J. H. *J. Comput. Aided Mol. Des.* **2000**, *14*, 123.